Published in final edited form as:
Cell. 2014 November 20; 159(5): 1070–1085. doi:10.1016/j.cell.2014.10.031.

Proinflammatory signaling regulates hematopoietic stem cell emergence

Raquel Espín-Palazón[1], **David L. Stachura**[1,2], **Clyde A. Campbell**[1], **Diana García-Moreno**[3], **Natasha Del Cid**[1], **Albert D. Kim**[1], **Sergio Candel**[3], **José Meseguer**[3], **Victoriano Mulero**[3,5], and **David Traver**[1,4,5]

[1]Department of Cellular and Molecular Medicine, University of California at San Diego, 9500 Gilman Drive, Natural Sciences Building 6107, La Jolla, CA 92093, USA

[3]Departamento de Biología Celular e Histología, Facultad de Biología, Universidad de Murcia, IMIB-Arrixaca, Campus Universitario de Espinardo, Murcia 30100, Spain

[4]Section of Cell and Developmental Biology, University of California at San Diego, La Jolla, CA, USA

Summary

Hematopoietic stem cells (HSCs) underlie the production of blood and immune cells for the lifetime of an organism. In vertebrate embryos, HSCs arise from the unique transdifferentiation of hemogenic endothelium comprising the floor of the dorsal aorta during a brief developmental window. To date, this process has not been replicated *in vitro* from pluripotent precursors, partly because the full complement of required signaling inputs remains to be determined. Here, we show that TNFR2 via TNFα activates the Notch and NF-κB signaling pathways to establish HSC fate, indicating a requirement for inflammatory signaling in HSC generation. We determine that primitive neutrophils are the major source of TNFα, assigning a role for transient innate immune cells in establishing the HSC program. These results demonstrate that proinflammatory signaling, in the absence of infection, is utilized by the developing embryo to generate the lineal precursors of the adult hematopoietic system.

[5]Corresponding Authors: dtraver@ucsd.edu, vmulero@um.es.
[2]Current address: Department of Biological Sciences, California State University, 400 West First Street, Chico 95929-0515 CA, USA

Author contributions

All studies presented herein derive from initial observations by R.E.-P. in the laboratory of V.M. R.E.-P, D.L.S., C.A.C., N.D.C., A. D. K, J. M., D.T., and V.M. designed experiments; R.E.-P., D.L.S, C.A.C., D.G.-M., N.D.C. and S.C. performed research; R.E.-P., D.L.S, C.A.C., D.G-M., N.D.C., A. D. K, S.C., J. M., V.M., and D.T. analyzed data; and R.E.-P., D.L.S., V.M., and D.T. wrote the paper with minor contributions from remaining authors.

Conflict of interest

The authors declare no conflicts of interest.

Introduction

In all vertebrate animals studied, the homeostasis of adult blood and immune cells is ultimately maintained by rare subsets of HSCs (Kondo et al., 2003). During a brief window during embryonic development, these HSCs arise *de novo* from hemogenic endothelium comprising the floor of the dorsal aorta (DA) (Bertrand et al., 2010a; Boisset et al., 2010; de Bruijn et al., 2000; Kissa and Herbomel, 2010) in a process that appears to be conserved among all vertebrates (Clements and Traver, 2013; Godin and Cumano, 2002). A more complete understanding of the signaling pathways that instruct HSC emergence could in principle inform *in vitro* approaches utilizing pluripotent precursors to create patient-specific HSCs (Kyba and Daley, 2003). Despite decades of efforts, this goal has not yet been achieved, in part due to an incomplete understanding of the native molecular cues needed to establish HSC fate.

One known requirement for HSC emergence is signaling through the Notch pathway (Bigas et al., 2013). Notch regulates many forms of intercellular communication, underlying many cell fate decisions including key roles in embryonic pattering (Kopan and Ilagan, 2009). Although the role of Notch in the maintenance and function of adult HSCs appears to be dispensable (Bigas and Espinosa, 2012), Notch signaling is absolutely required in the embryonic specification of HSCs in both the mouse (Bigas and Espinosa, 2012) and zebrafish (Bertrand et al., 2010b). In mice, the Notch receptor Notch1 (Kumano et al., 2003) and the Notch ligand Jagged1 (Jag1) are required for HSC specification (Bigas et al., 2010). It is important to note that, because Notch signaling is also indispensable for arterial specification (Quillien et al., 2014), and because HSCs derive directly from the aortic floor, it has been difficult to distinguish if Notch signaling regulates HSC emergence independently from its role in upstream arterial specification. Recent studies in Jag1-deficient mice have demonstrated HSC defects in the presence of normal arterial development, suggesting that these Notch requirements may be distinct and separable. Recent studies have also demonstrated that Notch signaling is required intrinsically within HSCs or their precursors (Robert-Moreno et al., 2008) via function of the Notch1 receptor (Hadland et al., 2004), suggesting that Jag1 may be a specific ligand of Notch1 in the specification of HSCs.

Tumor necrosis factor α (TNFα) is a powerful proinflammatory cytokine that plays a pivotal role in the regulation of inflammation and immunity. TNFα exerts its functions via engagement of one of two specific cell surface receptors (TNFRs), namely the 55 kDa TNFR1 (also known as TNFRSF1A) and the 75 kDa TNFR2 (also known as TNFRSF1B) (Shalaby et al., 1990). TNFR1 is expressed in most cell types, whereas TNFR2 is restricted to immune and endothelial cells (Aggarwal, 2003). Whereas TNFα signaling regulates aspects of adult hematopoiesis (Mizrahi and Askenasy, 2014), a potential role in the developmental specification of HSCs has not been addressed. However, it has been reported that TNFα and its receptors are highly expressed in the murine yolk sac and fetal liver, suggesting a possible role for this inflammatory cytokine in embryonic hematopoiesis (Kohchi et al., 1994).

Nuclear factor-kappa B (NF-κB) is a ubiquitous, inducible transcription factor that is activated by a diverse number of stimuli, including TNFα (Ahn and Aggarwal, 2005; Brown et al., 2008). A multitude of downstream targets, as well as upstream inducers, position NF-κB as a general sensor of cell stress. TNFα, signaling through TNFR2, is a well-known activator of NF-κB (Aggarwal et al., 2012; Faustman and Davis, 2010). TNFα activates NF-κB through its canonical pathway, in which IκBs (NF-κB inhibitors) are phosphorylated, ubiquitinated, and degraded, releasing NF-κB dimers that then translocate to the nucleus to bind specific NF-κB DNA binding sites to activate gene expression (Brown et al., 2008). A direct role of NF-κB in HSCs has not been extensively studied, although recent reports indicate that NF-κB positively regulates the transcription of genes involved in the maintenance and homeostasis of hematopoietic stem and progenitor cells (HSPCs) (Stein and Baldwin, 2013), as well as their microenvironmental interactions (Zhao et al., 2012). Whether or not NF-κB is important in HSC emergence has not been investigated.

TNFα and TNFRs (Tnfa and Tnfrs utilizing zebrafish nomenclature) are well-conserved in all vertebrate organisms (Wiens and Glenney, 2011), and we previously demonstrated that zebrafish Tnfa interacts with Tnfr1 and Tnfr2 (Espin et al., 2013). Recent studies in the zebrafish indicate that zebrafish Tnfa functions as a proinflammatory cytokine by activating endothelial cells (Roca et al., 2008). Additionally, the genetic inhibition of Tnfrs identified an essential role for Tnfa signaling in the development and maintenance of endothelial cells (Espin et al., 2013). Since HSCs arise from hemogenic endothelial cells, we queried if TNF signaling plays a role in HSC emergence. In the present study, we demonstrate a previously unappreciated requirement for TNF signaling in the generation of HSCs. We also show that NF-κB is active in nascent HSCs, and that this activation is essential for HSC emergence. Finally, we identify primitive neutrophils as a key source of Tnfa, assigning these cells a previously unidentified role in HSC development. In summary, we report an important role for inflammatory signaling in the birth of the adult hematopoietic system that is mediated by the proinflammatory cytokine Tnfa, the inflammatory transcription factor NF-κB, and the Notch signaling pathway under non-pathogenic conditions.

Results

Tnfa signaling through Tnfr2 is required for definitive, but not primitive, hematopoiesis

We previously demonstrated that Tnfa is required for embryonic blood vessel development (Espin et al., 2013). Since HSCs are generated from arterial vessels in the embryo (Bigas et al., 2013), we investigated if this proinflammatory cytokine also played a role in HSC development. To address this question, we isolated *kdrl*$^{+}$ endothelial cells by fluorescence activated cell sorting (FACS) from 26 hours post fertilization (hpf) transgenic *kdrl:mcherry* embryos and performed quantitative PCR (qPCR) for *tnfr1* and *tnfr2*. Both transcripts were enriched in these cells compared to the whole embryo (Fig. S1A). Sorted cells expressed high levels of endogenous *kdrl*, and were negative for the muscle-specific *myod* gene, demonstrating the purity of the sorted cells (Fig. S1B). To investigate if Tnfa signaling was required for HSC specification, we performed loss-of-function experiments for Tnfa and its two receptors, Tnfr1 and Tnfr2, utilizing specific antisense morpholinos (MOs) (Espin et al., 2013). In the zebrafish embryo, HSCs can be visualized along the axial vessels by

expression of *cmyb* using whole-mount *in situ* hybridization (WISH) (Burns et al., 2005). The number of *cmyb*$^+$ cells in or near the floor of the DA was significantly reduced in Tnfa- and Tnfr2-deficient embryos compared with their wild type (wt) siblings (Figs. 1A and 1B). However, loss of Tnfr1 showed no effect on HSC number, and its simultaneous depletion with Tnfr2 was not significantly different than loss of Tnfr2 alone (Figs. 1A and 1B), indicating that the action of Tnfa through Tnfr2, but not Tnfr1, is important in HSC development. This result was supported by quantitation of *cd41:eGFP*$^+$ HSPCs (Bertrand et al., 2008) using flow cytometry, which were significantly decreased in Tnfr2- and Tnfa-deficient fish at 3 days post fertilization (dpf) (Fig. 1C).

To further confirm the reduction of HSCs in Tnfr2- and Tnfa-deficient embryos, we directly visualized emerging HSCs from the floor of the DA in *kdrl:mCherry; cmyb:eGFP* double transgenic embryos (Bertrand et al., 2010a) at 48hpf by confocal microscopy (Fig. 1D). Consistent with the results above, the number of double positive *kdrl*$^+$*; cmyb*$^+$ HSCs in the floor of the DA was reduced approximately 50% when compared to control embryos (Figs. 1D and 1E), unaffected in Tnfr1 deficient embryos, and showed a similar 50% decrease in Tnfr1+Tnfr2 double depleted embryos (Fig. S1C). These reductions could be due to a defect in the initial specification of HSCs, or in their subsequent maintenance. To distinguish between these possibilities, we performed WISH for the nascent HSC marker *runx1* at earlier time points. Both Tnfr2- and Tnfa- deficient embryos showed significant reduction in the number of *runx1*$^+$ cells in the aortic floor at 24, 28, and 36 hpf (Figs. S1D and S1E), indicating that the functions of Tnfa and Tnfr2 are important during the earliest steps of HSC specification.

We next examined subsequent developmental stages for possible roles of Tnfa in the maintenance of nascent HSCs. To determine if Tnf receptors expression is modulated following HSC specification, we purified *kdrl*$^+$*; cmyb*$^-$ endothelial cells and *kdrl*$^+$*; cmyb*$^+$ HSCs from 48hpf *kdrl:mCherry; cmyb:eGFP* embryos by FACS. qPCR analysis showed that whereas *tnfr1* mRNA levels were similar in HSCs and endothelial cells, *tnfr2* transcripts markedly increased in HSCs (Fig. 1F). As this result suggested that Tnfr2 may play a role in HSC maintenance, we analyzed changes in HSC number in individual embryos over time. The number of *cmyb*$^+$*; kdrl*$^+$ cells in wild type animals expanded between 36 and 48 hpf, whereas Tnfr2- or Tnfa-deficient siblings showed similar numbers of HSCs at either timepoint (Figs. 1G–H). Together, these results suggest that Tnfa signaling through Tnfr2 is important both in the first steps of HSC specification and in their subsequent maintenance following emergence from the aortic endothelium. Finally, we examined later larval stages by monitoring the expression of *rag1* and *lck*, two genes expressed in developing thymocytes (Langenau et al., 2004), since the T cell lineage derives exclusively from HSCs (Bertrand et al., 2008; Gering and Patient, 2005). Expression of *rag1* was completely or nearly absent, respectively, in Tnfr2- and Tnfa-deficient animals at 4 dpf (Fig. 1I). However, the thymic anlage developed normally in all morphants, assessed by the expression of the thymic epithelial marker *foxn1* (Fig. 1J). These results were further verified utilizing *lck:eGFP* transgenic animals to track T cell development (Langenau et al., 2004). T cells were absent in Tnfr2- and Tnfa- deficient larvae at 4 dpf, whereas Tnfr1-deficient siblings showed normal T cell development (Fig. S1F). Together, these results indicate that Tnfa

signals via Tnfr2, and that this signaling pathway is important both for early specification and subsequent maintenance of HSC fate, such that the lineage is apparently lost by 4 dpf.

To further dissect the role of Tnfa signaling in hematopoiesis, we assessed if Tnfa and its receptors were required for the first waves of hematopoiesis, commonly referred to as "primitive" due to the transience of these cells and lack of upstream multipotent progenitors. In zebrafish, primitive hematopoiesis generates macrophages, neutrophils, and erythrocytes. The expression of *csf1ra*, a specific marker of macrophages (Herbomel et al., 2001), was unaffected in Tnfa-, Tnfr1-, and Tnfr2-deficient embryos at 24 hpf (Fig. S1G). Additionally, primitive neutrophils were unaffected at 30 hpf, as assayed using transgenic *mpx:eGFP* animals (data not shown). Similarly, primitive erythropoiesis, assessed by expression of the erythroid-specific transcription factor *gata1a* at 24 hpf, was unaffected in morphant embryos (Fig. S1G). Overall, these results indicated that Tnfa signaling was dispensable for primitive hematopoiesis and indispensable for definitive hematopoiesis in the zebrafish embryo.

Tnfr2- and Tnfa-deficient embryos display normal vasculogenesis

Because HSCs originate in arterial vessels, many mutants with vascular or arterial specification defects also have hematopoietic defects (Bigas and Espinosa, 2012). No vascular abnormalities were observed in Tnfr2- or Tnfa-deficient embryos at 24 hpf when assayed by WISH for the endothelial marker *kdrl* at the MO doses used in this study (Fig. 2A), and circulation was normal (*gata1:DsRed*$^{+}$, red blood cells) but reduced numbers of HSPCs and thrombocytes (*cd41:eGFP*$^{+}$)at 3 dpf (Fig. 2B). These results suggest that the functions of Tnfr2 and Tnfa are required specifically during HSC development independently of their role in developing vasculature. Thus, we could uncouple the vascular defects previously described for Tnfr2 (Espin et al., 2013) from its effects on HSC development using lower doses of Tnfr2 MO.

To address if HSC defects in Tnfr2- and Tnfa-deficient animals were a consequence of impaired arterial specification, we performed WISH for the arterial markers *efnb2a*, *dlc*, *notch1b*, and *notch3* (Lawson et al., 2001) in morphant embryos at 28 hpf. We observed no alterations in transcript levels when compared to control siblings (Fig. 2C). Taken together, these data indicate that Tnfa signaling through Tnfr2 is specifically required for HSC development.

Tnfr2 is intrinsically required for HSC development

Since Tnfr2 is expressed in endothelial cells (Figure S1A), we hypothesized that Tnfr2 is intrinsically required within the vascular lineage for HSC development. To test this hypothesis, we generated a transgenic zebrafish line in which the wt form of *tnfr2* is upregulated via induction of the Gal4 transcriptional transactivator. HSC development was observed by confocal microscopy following overexpression of Tnfr2 specifically within the vasculature in *fli1a:Gal4; UAS:RFP; cmyb:GFP; UAS:tnfr2* animals. The number of RFP^{+}GFP^{+} HSCs in quadruple transgenic embryos was significantly increased compared to their Tnfr2^{-} siblings (Figure 2D–E), demonstrating that Tnfr2 activity induces or supports the HSC program following targeted expression to the vasculature.

To verify that the loss of HSCs in Tnfr2 morphants was not due to the apoptosis of endothelial cells, we performed a TUNEL assay and immunohistochemistry for GFP in *kdrl:GFP* embryos injected with Tnfr2 MO. Analysis of endothelial cells by confocal microscopy at 28 hpf indicated that loss of Tnfr2 caused no increased apoptotic endothelial cells within the DA (Figure S2A), even though there was an increase in apoptotic non-endothelial cells. As a positive control for apoptosis in control animals, we imaged the lens of the eye (Cole and Ross, 2001) (Figure S2B). We also performed WISH for *runx1* in the same experiment to verify the reduction of HSCs in these embryos (Figures S2C–D). These results, together with the findings that there are no detectable apoptotic endothelial cells in the DA at 28 hpf (Kobayashi et al., 2014) indicate that the HSC specification defect in Tnfr2 deficient embryos is not caused by apoptosis induced by alterations of Tnfr1/Tnfr2 ratios within the vasculature.

Tnfa signaling acts upstream of Notch during HSC specification

During Notch activation, Notch receptors are stimulated by ligands from neighboring cells, triggering the cleavage of the Notch intracellular domain (NICD), which enters the nucleus to function as transcription factor essential for cell fate decisions (Lai, 2004). There are four Notch receptors (Notch1a, 1b, 2, and 3), five Delta family ligands (Dla, Dlb, Dlc, Dld, and Dll4) and three Jagged ligands (Jagged 1a, Jagged 1b, and Jagged 2) in zebrafish. Since TNFα activates the Notch pathway in certain contexts (Fernandez et al., 2008; Wang et al., 2013) we queried if signaling through Tnfr2 may similarly activate Notch signaling to specify HSCs. We performed loss-of-function experiments for Tnfr2 and Tnfa in transgenic *tp1:eGFP* animals, in which GFP is expressed by cells having recently experienced Notch signaling (Parsons et al., 2009). Consistent with our other findings, the depletion of either Tnfa or Tnfr2 led to a two-fold reduction in *tp1:eGFP*$^{+}$*; kdrl:mCherry*$^{+}$ HSPCs in the aortic floor at 26 hpf (Fig. 3A arrowheads and 3B). These observations indicated that Tnfr2 signaling was upstream of Notch signaling during HSC specification.

If Notch signaling is indeed required downstream of Tnfr2 function for HSC specification, then ectopic expression of the Notch1a intracellular domain (NICD1a) should rescue the lack of HSCs in Tnfr2- and Tnfa-deficient embryos. We performed two different experiments to address the timing and tissue specificity of this Tnfa-dependent Notch requirement. To provide temporal control of NICD1a induction, we utilized inducible *hsp70:Gal4; UAS:NICD1a-myc* double transgenic embryos, which express NICD1a under the control of the inducible Gal4 system. Induction of NICD1a at 18 hpf rescued the depletion of *runx1*$^{+}$ HSCs at 28 hpf along the DA in both Tnfa and Tnfr2 morphants (Fig. 3C). We then enforced the expression of NICD1a within endothelial cells utilizing *kdrl:Gal4; UAS:NICD1a-myc* double transgenic embryos that had been injected with Tnfr2 or Tnfa MOs. Endothelial expression of NICD1a restored *runx1*$^{+}$ cells along the aortic floor (Fig. 3D), indicating that TNF signaling activates the Notch pathway within hemogenic endothelium to specify HSC fate.

Tnfa induces Jag1a within endothelial cells to promote HSC specification through Notch1a

We next investigated potential mechanisms by which Tnfa and Tnfr2 induced Notch activation. Due to the fact that Tnfa signaling has been reported to induce or inhibit the

expression of specific Notch ligands (Fernandez et al., 2008; Sainson et al., 2008), we analyzed expression of the eight zebrafish Notch ligands within purified *kdrl*$^{+}$ endothelial cells from Tnfr2-deficient embryos. Only *jagged1a* expression was down-regulated in Tnfr2 morphants relative to controls (Fig. 4A). Using a *fli1a:Gal4* driver to enforce expression of Tnfr2 specifically within the vasculature, we examined Notch ligand expression in *fli1a:Gal4; UAS:tnfr2* animals by qPCR (Fig. 4B). We detected a 20-fold -increase of *tnfr2* in *UAS:Tnfr2*$^{+}$ compared to *UAS:Tnfr2*$^{-}$ embryos (Fig. 4B). Consistent with our previous results, only *jag1a* mRNA levels were increased following the enforced expression of Tnfr2 (Fig. 4B).

Interestingly, Jag1 is required for the generation of definitive hematopoietic cells in mice, but dispensable for arterial development. A potential role for Jag1 in zebrafish HSPC development has not been addressed. Two paralogues of the single *JAG1* human gene are present in the zebrafish genome: *jag1a* and *jag1b*. Since only *jag1a* levels were modulated by Tnfr2, we performed loss-of-function experiments with this gene. Loss of *jag1a* led to decreased HSC numbers as analyzed by *runx1* expression along the DA (Fig. 4C). However, specification of aortic fate was normal, as *efnb2a* and *dlc* levels were unperturbed (Fig. 4C). To further verify that Tnfr2 and Jag1a were in the same genetic pathway, we performed synergy studies by co-injecting low doses of Tnfr2 and Jag1a MOs simultaneously. Aortic *runx1*$^{+}$ cells were significantly reduced in Tnfr2- and Jag1a- double-deficient embryos compared to single-deficient embryos (Fig. 4D). Tnfr2 function thus lies genetically upstream of *jag1a* during HSC specification. To investigate potential Jag1a-presenting cells, we isolated *cmyb*$^{-}$, *kdrl*$^{+}$ endothelial cells and *cmyb*$^{+}$, *kdrl*$^{+}$ HSCs for qPCR analysis of *jag1a* at 48 hpf. *jag1a* transcripts were 4-fold more abundant in endothelial cells than in HSCs (Fig. S3), suggesting that Notch signaling in HSCs or hemogenic endothelium is activated by neighboring Jag1a^{+} endothelial cells.

We next investigated which of the four Notch receptors were downstream of Jag1a during HSC induction. In the mouse, Notch1 is required within HSCs or their lineal precursors to instruct HSC fate. We therefore focused upon the two zebrafish orthologues of human NOTCH1, Notch1a and Notch1b. To investigate if either receptor functioned downstream of Tnfr2 to specify HSCs, we performed synergy experiments by co-injecting low doses of Tnfr2 MO with morpholinos against Notch1a or Notch1b. Only the simultaneous depletion of Tnfr2 and Notch1a, but not Tnfr2 and Notch1b, led to a statistically significant decrease in *runx1* expression compared to single morphants at 28 hpf (Fig. 4E). This finding suggests that Notch1a serves as the Notch receptor for Jag1a to specify HSC fate downstream of Tnfr2.

The proinflammatory transcription factor NF-κB is active in emerging HSCs

Activation of TNF receptors by ligand binding leads to the recruitment of adaptor proteins that trigger NF-κB activation (Aggarwal et al., 2012). Moreover, the induction of *jag1* transcription by Tnfa in murine endothelial cells is NF-κB dependent (Johnston et al., 2009). Interestingly, NF-κB (as well as Tnfr2 and Jag1) is necessary for embryonic vessel development (Santoro et al., 2007). These lines of evidence suggested that NF-κB could have a previously unappreciated role in HSC specification, prompted us to examine its role

in HSC development. We utilized an NF-κB activation reporter transgenic line (Kanther et al., 2011), in combination with the *kdrl:mcherry* transgene to perform confocal analysis of the DA at different time points. Interestingly, we observed NF-κB^{high} cells in the floor of the DA at 24 hpf, typically in pairs and in direct contact with each other (Fig. 5A). We also observed NF-κB^{+} cells along the roof of the DA, but a much lower frequency than in the floor (data not shown). *NF-κB*$^{+}$, *kdrl*$^{+}$ cells remained visible at 30 hpf (Fig. 5A), and underwent endothelial-to-hematopoietic transition (EHT) (Supplementary video S1), a characteristic feature of emerging HSCs. To further evaluate if HSCs had increased NF-κB activation compared to their surrounding endothelial neighbors, *kdrl*$^{+}$*; cmyb*$^{+}$ HSCs and *kdrl*$^{+}$*; cmyb*$^{-}$ endothelial cells were isolated from 48 hpf *kdrl:mCherry; cmyb:eGFP* embryos by FACS for qPCR analyses. Whereas endothelial cells had 20- to 30-fold induction of the NF-κB response genes interleukin 1 beta (*il1b*) and nuclear factor of kappa light polypeptide gene enhancer in B-cells inhibitor alpha a (*ikbaa*) relative to whole embryo expression, HSCs displayed 300- and 2300-fold increases in *il1b* and *ikbaa*, respectively (Fig. 5B). Immunohistochemistry for the NF-κB subunit p65 in *kdrl:mcherry* embryos showed that, although p65 was detected in the cytoplasm of every cell as expected, it was more intense in the pronephros (Fig. 5C–D, yellow asterisks), in the DA, and in cells potentially undergoing the endothelial to hematopoietic transition in the aortic floor (Fig. 5C–D, arrow). These results indicate that NF-κB activation is a characteristic feature of emerging HSCs.

Multiple lines of evidence support the integration of the Notch and NF-κB signaling pathways during the differentiation of various cell types (Ang and Tergaonkar, 2007; Cao et al., 2011; Espinosa et al., 2010; Espinosa et al., 2003; Shin et al., 2006; Song et al., 2008). For this reason, we investigated if NF-κB^{+} cells in the floor of the DA also had active Notch signaling, utilizing double transgenic *tp1:nlsCherry; NFKB:GFP* animals to simultaneously visualize respective Notch and NF-κB-activation. NF-κB^{+} cells in the floor of the DA were also tp1^{+} (Fig. 5C). No NFKB^{+}, tp1^{-} cells were found in the floor of the DA, suggesting that Notch is (or was previously) active in NF-κB^{+} HSPCs.

NF-κB activation is required for HSC specification and acts downstream of Tnfr2

To determine if NF-κB function is required for HSC emergence we developed a Tg(*UAS:dn-ikbaa*) transgenic animal that functions as a dominant negative inhibitor of NF-κB (Fig. S4A, B). Similar truncation constructs have been utilized *in vitro* to inhibit NF-κB activation (Abbas and Abu-Amer, 2003). At 6 hours post heat-shock in *hsp70:Gal4; UAS:dn-ikbaa* animals, *dn-ikbaa* mRNA levels were detected in *dn-ikbaa*$^{+}$ but not in *dn-ikbaa*$^{-}$ siblings (Fig. S4C). qPCR for the NF-κB response gene *il1b* in FACS-purified *fli1a*$^{+}$ endothelial cells showed significant downregulation in the *dn-ikbaa*$^{+}$ embryos compared to their *dn-ikbaa*$^{-}$ siblings (Fig. S4D, E). Lipopolysaccharide (LPS) challenge of wt embryos produced a significant increase in *il1b* expression compared to phosphate-buffered saline-(PBS) injected controls, as previously described (van der Vaart et al., 2013), but not in *dn-ikbaa*$^{+}$ embryos (Figure S4F, G), indicating that *dn-ikbaa*$^{+}$ embryos are unable to trigger an inflammatory response through NF-κB. These results thus demonstrate that *UAS:dn-ikbaa* embryos have impaired NF-κB activation.

Blockade of NF-κB function at 20 hpf in *hsp70:Gal4; UAS:dn-ikbaa* animals led to loss of HSCs at 48hpf (Fig. 6A). Loss of NF-κB specifically within the vasculature using *fli1a*:Gal4; *UAS:dn-ikbaa* double transgenic embryos also led to a depletion of *cmyb*$^+$ cells (Fig. 6B). qPCR for *il1b* in FACS-purified endothelial cells showed a threefold decrease in Tnfr2 morphants (Fig. 6C), demonstrating that NF-κB acts downstream of Tnfr2 during HSC specification. Together, these results suggest that NF-kB activation in hemogenic endothelium is a key event in the specification of HSCs.

Primitive neutrophils are the key source of Tnfa

In adult organisms, immune cells are the main source of TNFα, including T and B lymphocytes, macrophages and neutrophils (Aggarwal, 2003). From 22 to 72 hpf, the temporal window over which zebrafish HSCs emerge from aortic endothelium, the only leukocytes present are primitive myeloid cells, namely macrophages and neutrophils (Herbomel et al., 1999; Le Guyader et al., 2008). Interestingly, *tnfa* expression in the zebrafish embryo was not detectable during the first 9 hours of development, but was expressed before 24 hpf (Espin et al., 2013), when HSCs are initially specified (Clements and Traver, 2013). We therefore hypothesized that primitive myeloid cells were the source of Tnfa. We isolated *mpeg:GFP*$^+$ primitive macrophages and *mpx:GFP*$^+$ primitive neutrophils by FACS at two different timepoints and performed qPCR for *tnfa* (Fig. 7A). Although both populations expressed *tnfa*, the highest expression was observed within the neutrophil fraction (Fig. 7A). We then utilized a pU.1 MO to specifically ablate both primitive myeloid lineages *in vivo* (Rhodes et al., 2005). pu1 MO efficacy was validated by WISH using the pan-leukocyte marker *l-plastin* and the neutrophil marker *mpx* at 48 hpf (Fig. S5A). Following ablation of primitive myeloid cells in pu1 morphants, HSCs were enumerated by confocal microscopy of *kdrl*$^+$*cmyb*$^+$ cells. A two-fold decrease in HSC number was detected in pu1 morphants compared to their control siblings (Fig. 7B–C). To elucidate which primitive myeloid population was responsible for the decrease in HSC number, we utilized an irf8 MO (Li et al., 2011), which skews myeloid development to almost entirely neutrophilic. Loss of the macrophage lineage was confirmed in irf8 morphants by qPCR for the macrophage-specific marker *mpeg1* (Fig. S5B). Surprisingly, the number of *kdrl*$^+$*; cmyb*$^+$ HSCs increased following loss of the macrophage lineage (Fig. 7D–E). In agreement with our *tnfa* expression data, this result suggests that neutrophils are the key source of the Tnfa needed for HSC emergence. To test this hypothesis, we quantified *tnfa* expression levels in pu1- and irf8-deficient animals. Expression of *tnfa* was consistently decreased following loss of pu1 function, and increased following loss of irf8 function (Fig. 7F). In addition, although *runx1* was upregulated in irf8-deficient embryos, the simultaneous depletion of Tnfa and Irf8 led to a marked reduction in *runx1* expression, despite the elevated numbers of neutrophils present (Fig. 7G). These findings demonstrate that production of Tnfa from primitive neutrophils is critical for the specification and/or maintenance of HSC fate.

Overall, these data indicate that production of Tnfa from primitive neutrophils activates Tnfr2, upregulating the expression of Jag1a on the surface of endothelial cells. Jag1a in turn activates Notch1a, triggering a signaling cascade whereby NF-κB triggers a transcriptional program required for the emergence of HSCs from hemogenic endothelium (Fig. S5C, D).

Discussion

Traditionally, infection and inflammation were thought to play an indirect role in HSC homeostasis by causing increased proliferation and skewed differentiation towards microbicidal immune cell lineages (Takizawa et al., 2012). However, recent studies indicate that HSCs can respond directly to the inflammatory cytokines interferon (IFN) α/β, γ and TNFα (Baldridge et al., 2011; King and Goodell, 2011). Additionally, there is evidence that HSCs can upregulate cytokines under stress-induced hematopoiesis (Zhao et al., 2014). Here, we examined a much earlier step in the biology of HSCs; their specification and emergence from hemogenic endothelium in the developing embryo. The emergence of HSCs from the aortic floor is transient, and occurs during developmental windows when the surrounding environment is relatively sterile, whether it is *in utero* in mammals, or within the chorion in teleosts. It is therefore surprising that a key pathway underlying the canonical response to infection and inflammation is required to generate the founders of the adult hematopoietic system. Our studies in the zebrafish demonstrate that depletion of Tnfa or its cognate receptor Tnfr2 leads to depletion of emerging HSCs. The key event elaborated by Tnfr2 appears to be activation of the Notch pathway, since ectopic provision of Notch signaling rescued HSCs in the absence of Tnfa or Tnfr2 function. While Notch signaling is required for HSC specification across vertebrate phyla, little is known regarding how this Notch event is regulated, or which of the many receptors or ligands are necessary to fate HSCs from ventral aortic endothelium.

That the HSC program can be rescued in either Tnfa or Tnfr2 morphants by enforced expression of NICD1a within the vasculature demonstrates that the TNF pathway lies upstream of Notch in HSC specification. Our results suggest that signaling via Tnfr2 specifically controls Notch activation by inducing the Notch ligand *jag1a* in cells within the DA. Synergy experiments depleting Notch1a and Tnfr2 combinatorially indicate that Notch1a is likely the receptor on HSCs that binds to the Jag1a ligand presented by aortic endothelial cells. These findings are consistent with studies in the mouse embryo, where Notch1 is required cell-autonomously within HSCs or their lineal precursors for their specification (Hadland et al., 2004; Kumano et al., 2003). The zebrafish Notch1a and Notch1b receptors are evolutionary paralogues of mammalian Notch1 (Kortschak et al., 2001), and are both expressed in the DA during the window of HSC emergence (Quillien et al., 2014). Our findings extend these results by demonstrating that Notch1 function is evolutionarily conserved in the specification of HSCs and provide a more detailed mechanism regarding how Notch1 may actually function in this process. Further studies will be required, however, to determine the precise interactions between Jag1a and Notch1a and how these interactions lead to establishment of HSC fate.

In addition to its regulation of the Notch pathway, our results also suggest that Tnfa signaling exerts its effects through NF-κB. Although NF-κB is known to play a key role in adult mammalian hematopoiesis (Gerondakis et al., 2012), a role in the embryonic emergence of HSCs has not been reported. The utilization of a *NFκB:GFP* reporter line allowed us to image the *in vivo* activation of NF-κB, indicating that this activation is required within endothelial cells of the DA for HSC emergence. Furthermore, these studies suggest that this activity is downstream of Tnfa/Tnfr2 signaling. Intriguingly, these data also

demonstrate that NF-κB$^+$ cells in the floor of the DA are often positive for Notch activity when assessed along with the *tp1* Notch reporter line. Whereas recent evidence suggests that Notch1 can modulate NF-κB activity in different cellular contexts, it remains to be determined whether one factor is epistatic to the other or if both may operate together within the hemogenic endothelium to establish HSC fate.

In this study, we have also discovered an unexpected role for neutrophils in HSC development. Whereas macrophages are involved in a broad array of developmental processes (Wynn et al., 2013), an active role for neutrophils in modulating developmental events has not been described. Here, we report for the first time that primitive neutrophils are a major source of Tnfa, and that the loss of either neutrophils or Tnfa results in the loss of developing HSCs. The prevailing view that primitive myeloid cells have evolved predominantly to provide early immunity is thus likely over simplistic. At any timepoint during HSC emergence, whether early during HSC specification or later during EHT, we observed approximate two-fold decreases in HSC number. That the lineal descendants of HSCs, most importantly T lymphocytes, are absent by 4–5 dpf indicates that the Tnfa/Tnfr2 signaling axis is required to sustain HSC function. Collectively, our findings suggest that activation of Tnfr2 is important both in hemogenic endothelium and in maintaining nascent HSC fate. It is important to note that *tnfa* is also expressed in endothelial cells (data not shown); contribution from the endothelium may thus play a role in either or both of these processes. The means to create conditional, tissue-specific gene disruption in the zebrafish will be required to precisely address the relative importance of each source.

In conclusion, we show that TNFα, a cytokine that has become the paradigm for induction of inflammatory responses, is also key in the establishment of the hematopoietic system through its influence on HSC formation in the developing embryo. In addition to the known signaling inputs required to establish HSC fate, inflammatory signals should now be added to this list. A major challenge for the field is to integrate each of these required inputs to better understand their spatial and temporal requirements, such that this knowledge may be utilized to instruct HSC fate *in vitro* from human pluripotent precursors, a major unrealized goal of regenerative medicine.

Experimental Procedures

Zebrafish husbandry and strains

Zebrafish embryos and adults were mated, staged, raised and processed as described (Westerfield, 2000) and maintained in accordance with UCSD IACUC guidelines. See Supplementary Procedures for description of transgenic lines.

Heat-shock treatment

For induction of *hsp70l:Gal4*-driven transgenes, embryos were placed in E3 medium and transferred to a 38°C water bath for 45 min at noted stages.

Generation of transgenic animals

Tg (*UAS:dnnfkbiaa*)^{sd35} *and Tg(UAS:Tnfr2)*^{ums1} embryos were generated by Tol2-mediated transgenesis via the multisite Gateway cloning system (Invitrogen). See also Supplemental Experimental Procedures.

Morpholino injection

Specific antisense targeting morpholinos (MOs) (Gene Tools) were resuspended in DEPC-treated water at 1–3mM and injected in one-cell stage embryos. See also Supplemental Experimental Procedures.

Enumeration of HSCs

Animals were subjected to WISH for *runx1* and *cmyb* at noted stages and positive cells were imaged and manually counted. Confocal microscopy was performed on *cmyb:GFP; kdrl:mcherry* double transgenic animals (Bertrand et al., 2010a), *tp1:eGFP; kdrl:mcherry* double transgenic animals, and *NF-κB:GFP; kdrl:mcherry* double transgenic animals. Z-sections of the DA region were captured on a Leica SP5 microscope (Leica) using Volocity Acquisition, Visualization, and Restoration software (Improvision), and manually counted.

Fluorescent visualization of blood flow, HSPCs, and T cells

To visualize blood flow and HSPCs, and T cells, *cd41:eGFP; gata1:dsred* embryos at 3 dpf and *lck:GFP* larvae at 4 dpf, respectively, were anesthetized in Tricaine (200 μg/ml) and examined using a Leica MZ16FA stereomicroscope.

Flow cytometry and fluorescence-activated cell sorting

Briefly, embryos were dechorionated with pronase, anesthetized in tricaine and dissociated with liberase or triturated with a P1000 pipette. The resulting suspension was filtered with a 40 μm cell strainer and flow cytometric acquisitions or FACS were performed on a FACS LSRII. See also Supplemental Experimental Procedures.

Whole-mount RNA in situ hybridization (WISH)

WISH was carried out as described (Thisse et al., 1993). Probes for the *gata1a*, *csfr1ra*, *kdrl*, *cmyb*, *runx1*, *foxn1*, *efnb2a*, *dlc*, *notch1b*, *notch3*, and *rag1* transcripts were generated using the DIG RNA Labeling Kit (Roche Applied Science) from linearized plasmids. *dn-ikbaa* probe was generated from bp 118-933 of *dn-IkBaa* (see Figure S2). Embryos were imaged using a Leica M165C stereomicroscope equipped with a DFC295 color digital camera (Leica) and FireCam software (Leica).

Statistical analysis

Data were analyzed by analysis of variance (ANOVA). In all figures, solid red bars denote the mean, and error bars represent S.E.M. * $p< 0.05$, ** $p < 0.01$, *** $p < 0.001$, n.s. not significant, n.d. not detected.

Quantitative RT-PCR analysis

RNA was isolated from tissues with RNeasy (Qiagen), and cDNA generated with qScript Supermix (Quanta BioSciences). Primers to detect zebrafish transcripts are described in Supplemental Table 1. Relative expression levels of genes were calculated by the following formula: Relative expression= $2^{-(Ct[\text{gene of interest}]-Ct[\text{housekeeping gene}])}$.

Immunofluorescence of NICD^{+} animals

The immunofluorescence staining for cMyc in *hsp70:gal4; UAS:NICD-myc* zebrafish embryos was performed as previously described (Kim et al., 2014).

Detection of apoptotic cell death by TUNEL labeling

The TUNEL assay was performed as previously described (Espin et al., 2013) with slight modifications. See also Supplemental Experimental Procedures.

Lipopolysaccharide injections

Tg(*hsp:Gal4; UAS:dn-ikbaa*) embryos were manually dechorionated at 24 hpf, followed by heat shock at 38°C for 50 minutes. Four hours post heat shock, 2 nl of PBS or LPS (900 μg/ml) (#L6511, Sigma) were injected into the posterior blood island (PBI). Embryos were then harvested one hour post injection (hpi) and RNA was isolated for qPCR analysis.

Microtome sections and immunohistochemistry

Embryos were fixed with 4% PFA, embedded in paraffin, and sectioned at 5 μm in thickness with Leica microtome. Immunohistochemistry was performed as previously described (Kobayashi et al., 2014). The following antibodies were used: mouse anti-mcherry 1:500 (Abcam, ab125096), rabbit anti-p65 (NF-κB) (RB-1638-P; Lab Vision) 1:200, donkey anti-rabbit IgG Alexa Fluor 594-conjugated (Molecular Probes, A-21207) 1:1000 and donkey anti-mouse IgG Alexa Fluor 488-conjugated (Molecular Probes, A-11029) in addition to DAPI 1:1000 (Life Technologies, D3571).

Supplementary Material

Refer to Web version on PubMed Central for supplementary material.

Acknowledgments

This work was supported by the Spanish Ministry of Science and Innovation (grant numbers BIO2008-01379, BIO2011-23400 and CSD2007-00002 to VM), the Fundación Séneca, Agencia Regional de Ciencia y Tecnología de la Región de Murcia (grant number 04538/GERM/06 to V.M. and predoctoral and postdoctoral fellowships to R.E-P), the NIH (K01-DK087814-01A1; D.L.S.), a CIRM New Faculty Award RN1-00575-1 (D.T.), AHA Innovative Science Award #12PILT12860010 (D.T.), and NIH R01-DK074482 (D.T.). We thank Inmaculada Fuentes, Pedro Martínez, Efren Reyes, Chase Melick and Karen Ong for technical assistance, Nadia Mercader for ideas and discussion, Francisco Juan Martínez-Navarro and Liangdao Li for his help with WISH, and Kylie Price and SAI staff for flow cytometry.

References

Abbas S, Abu-Amer Y. Dominant-negative IkappaB facilitates apoptosis of osteoclasts by tumor necrosis factor-alpha. J Biol Chem. 2003; 278:20077–20082. [PubMed: 12637573]

Aggarwal BB. Signalling pathways of the TNF superfamily: a double-edged sword. Nat Rev Immunol. 2003; 3:745–756. [PubMed: 12949498]

Aggarwal BB, Gupta SC, Kim JH. Historical perspectives on tumor necrosis factor and its superfamily: 25 years later, a golden journey. Blood. 2012; 119:651–665. [PubMed: 22053109]

Ahn KS, Aggarwal BB. Transcription factor NF-kappaB: a sensor for smoke and stress signals. Ann N Y Acad Sci. 2005; 1056:218–233. [PubMed: 16387690]

Ang HL, Tergaonkar V. Notch and NFkappaB signaling pathways: Do they collaborate in normal vertebrate brain development and function? Bioessays. 2007; 29:1039–1047. [PubMed: 17876798]

Baldridge MT, King KY, Goodell MA. Inflammatory signals regulate hematopoietic stem cells. Trends in immunology. 2011; 32:57–65. [PubMed: 21233016]

Bertrand JY, Chi NC, Santoso B, Teng S, Stainier DY, Traver D. Haematopoietic stem cells derive directly from aortic endothelium during development. Nature. 2010a; 464:108–111. [PubMed: 20154733]

Bertrand JY, Cisson JL, Stachura DL, Traver D. Notch signaling distinguishes 2 waves of definitive hematopoiesis in the zebrafish embryo. Blood. 2010b; 115:2777–2783. [PubMed: 20107232]

Bertrand JY, Kim AD, Teng S, Traver D. CD41+ cmyb+ precursors colonize the zebrafish pronephros by a novel migration route to initiate adult hematopoiesis. Development. 2008; 135:1853–1862. [PubMed: 18417622]

Bigas A, Espinosa L. Hematopoietic stem cells: to be or Notch to be. Blood. 2012; 119:3226–3235. [PubMed: 22308291]

Bigas A, Guiu J, Gama-Norton L. Notch and Wnt signaling in the emergence of hematopoietic stem cells. Blood Cells Mol Dis. 2013; 51:264–270. [PubMed: 23927968]

Bigas A, Robert-Moreno A, Espinosa L. The Notch pathway in the developing hematopoietic system. Int J Dev Biol. 2010; 54:1175–1188. [PubMed: 20711994]

Boisset JC, van Cappellen W, Andrieu-Soler C, Galjart N, Dzierzak E, Robin C. In vivo imaging of haematopoietic cells emerging from the mouse aortic endothelium. Nature. 2010; 464:116–120. [PubMed: 20154729]

Brown KD, Claudio E, Siebenlist U. The roles of the classical and alternative nuclear factor-kappaB pathways: potential implications for autoimmunity and rheumatoid arthritis. Arthritis Res Ther. 2008; 10:212. [PubMed: 18771589]

Burns CE, Traver D, Mayhall E, Shepard JL, Zon LI. Hematopoietic stem cell fate is established by the Notch-Runx pathway. Genes & development. 2005; 19:2331–2342. [PubMed: 16166372]

Cao Q, Kaur C, Wu CY, Lu J, Ling EA. Nuclear factor-kappa beta regulates Notch signaling in production of proinflammatory cytokines and nitric oxide in murine BV-2 microglial cells. Neuroscience. 2011; 192:140–154. [PubMed: 21729740]

Clements WK, Traver D. Signalling pathways that control vertebrate haematopoietic stem cell specification. Nat Rev Immunol. 2013; 13:336–348. [PubMed: 23618830]

Cole LK, Ross LS. Apoptosis in the developing zebrafish embryo. Dev Biol. 2001; 240:123–142. [PubMed: 11784051]

de Bruijn MF, Speck NA, Peeters MC, Dzierzak E. Definitive hematopoietic stem cells first develop within the major arterial regions of the mouse embryo. EMBO J. 2000; 19:2465–2474. [PubMed: 10835345]

Espin R, Roca FJ, Candel S, Sepulcre MP, Gonzalez-Rosa JM, Alcaraz-Perez F, Meseguer J, Cayuela ML, Mercader N, Mulero V. TNF receptors regulate vascular homeostasis in zebrafish through a caspase-8, caspase-2 and P53 apoptotic program that bypasses caspase-3. Dis Model Mech. 2013; 6:383–396. [PubMed: 22956347]

Espinosa L, Cathelin S, D'Altri T, Trimarchi T, Statnikov A, Guiu J, Rodilla V, Ingles-Esteve J, Nomdedeu J, Bellosillo B, et al. The Notch/Hes1 pathway sustains NF-kappaB activation through CYLD repression in T cell leukemia. Cancer cell. 2010; 18:268–281. [PubMed: 20832754]

Espinosa L, Ingles-Esteve J, Robert-Moreno A, Bigas A. IkappaBalpha and p65 regulate the cytoplasmic shuttling of nuclear corepressors: cross-talk between Notch and NFkappaB pathways. Mol Biol Cell. 2003; 14:491–502. [PubMed: 12589049]

Faustman D, Davis M. TNF receptor 2 pathway: drug target for autoimmune diseases. Nat Rev Drug Discov. 2010; 9:482–493. [PubMed: 20489699]

Fernandez L, Rodriguez S, Huang H, Chora A, Fernandes J, Mumaw C, Cruz E, Pollok K, Cristina F, Price JE, et al. Tumor necrosis factor-alpha and endothelial cells modulate Notch signaling in the bone marrow microenvironment during inflammation. Exp Hematol. 2008; 36:545–558. [PubMed: 18439488]

Gering M, Patient R. Hedgehog signaling is required for adult blood stem cell formation in zebrafish embryos. Dev Cell. 2005; 8:389–400. [PubMed: 15737934]

Gerondakis S, Banerjee A, Grigoriadis G, Vasanthakumar A, Gugasyan R, Sidwell T, Grumont RJ. NF-kappaB subunit specificity in hemopoiesis. Immunol Rev. 2012; 246:272–285. [PubMed: 22435561]

Godin I, Cumano A. The hare and the tortoise: an embryonic haematopoietic race. Nat Rev Immunol. 2002; 2:593–604. [PubMed: 12154378]

Hadland BK, Huppert SS, Kanungo J, Xue Y, Jiang R, Gridley T, Conlon RA, Cheng AM, Kopan R, Longmore GD. A requirement for Notch1 distinguishes 2 phases of definitive hematopoiesis during development. Blood. 2004; 104:3097–3105. [PubMed: 15251982]

Herbomel P, Thisse B, Thisse C. Ontogeny and behaviour of early macrophages in the zebrafish embryo. Development. 1999; 126:3735–3745. [PubMed: 10433904]

Herbomel P, Thisse B, Thisse C. Zebrafish early macrophages colonize cephalic mesenchyme and developing brain, retina, and epidermis through a M-CSF receptor-dependent invasive process. Dev Biol. 2001; 238:274–288. [PubMed: 11784010]

Johnston DA, Dong B, Hughes CC. TNF induction of jagged-1 in endothelial cells is NFkappaB-dependent. Gene. 2009; 435:36–44. [PubMed: 19393188]

Kanther M, Sun X, Muhlbauer M, Mackey LC, Flynn EJ 3rd, Bagnat M, Jobin C, Rawls JF. Microbial colonization induces dynamic temporal and spatial patterns of NF-kappaB activation in the zebrafish digestive tract. Gastroenterology. 2011; 141:197–207. [PubMed: 21439961]

Kim AD, Melick CH, Clements WK, Stachura DL, Distel M, Panakova D, MacRae C, Mork LA, Crump JG, Traver D. Discrete Notch signaling requirements in the specification of hematopoietic stem cells. EMBO J. 2014

King KY, Goodell MA. Inflammatory modulation of HSCs: viewing the HSC as a foundation for the immune response. Nat Rev Immunol. 2011; 11:685–692. [PubMed: 21904387]

Kissa K, Herbomel P. Blood stem cells emerge from aortic endothelium by a novel type of cell transition. Nature. 2010; 464:112–115. [PubMed: 20154732]

Kobayashi I, Kobayashi-Sun J, Kim AD, Pouget C, Fujita N, Suda T, Traver D. Jam1a-Jam2a interactions regulate haematopoietic stem cell fate through Notch signalling. Nature. 2014; 512:319–323. [PubMed: 25119047]

Kohchi C, Noguchi K, Tanabe Y, Mizuno D, Soma G. Constitutive expression of TNF-alpha and -beta genes in mouse embryo: roles of cytokines as regulator and effector on development. The International journal of biochemistry. 1994; 26:111–119. [PubMed: 8138038]

Kondo M, Wagers AJ, Manz MG, Prohaska SS, Scherer DC, Beilhack GF, Shizuru JA, Weissman IL. Biology of hematopoietic stem cells and progenitors: implications for clinical application. Annual review of immunology. 2003; 21:759–806.

Kopan R, Ilagan MX. The canonical Notch signaling pathway: unfolding the activation mechanism. Cell. 2009; 137:216–233. [PubMed: 19379690]

Kortschak RD, Tamme R, Lardelli M. Evolutionary analysis of vertebrate Notch genes. Dev Genes Evol. 2001; 211:350–354. [PubMed: 11466531]

Kumano K, Chiba S, Kunisato A, Sata M, Saito T, Nakagami-Yamaguchi E, Yamaguchi T, Masuda S, Shimizu K, Takahashi T, et al. Notch1 but not Notch2 is essential for generating hematopoietic stem cells from endothelial cells. Immunity. 2003; 18:699–711. [PubMed: 12753746]

Kyba M, Daley GQ. Hematopoiesis from embryonic stem cells: lessons from and for ontogeny. Exp Hematol. 2003; 31:994–1006. [PubMed: 14585361]

Lai EC. Notch signaling: control of cell communication and cell fate. Development. 2004; 131:965–973. [PubMed: 14973298]

Langenau DM, Ferrando AA, Traver D, Kutok JL, Hezel JP, Kanki JP, Zon LI, Look AT, Trede NS. In vivo tracking of T cell development, ablation, and engraftment in transgenic zebrafish. Proc Natl Acad Sci U S A. 2004; 101:7369–7374. [PubMed: 15123839]

Lawson ND, Scheer N, Pham VN, Kim CH, Chitnis AB, Campos-Ortega JA, Weinstein BM. Notch signaling is required for arterial-venous differentiation during embryonic vascular development. Development. 2001; 128:3675–3683. [PubMed: 11585794]

Le Guyader D, Redd MJ, Colucci-Guyon E, Murayama E, Kissa K, Briolat V, Mordelet E, Zapata A, Shinomiya H, Herbomel P. Origins and unconventional behavior of neutrophils in developing zebrafish. Blood. 2008; 111:132–141. [PubMed: 17875807]

Li L, Jin H, Xu J, Shi Y, Wen Z. Irf8 regulates macrophage versus neutrophil fate during zebrafish primitive myelopoiesis. Blood. 2011; 117:1359–1369. [PubMed: 21079149]

Mizrahi K, Askenasy N. Physiological functions of TNF family receptor/ligand interactions in hematopoiesis and transplantation. Blood. 2014; 124:176–183. [PubMed: 24859365]

Parsons MJ, Pisharath H, Yusuff S, Moore JC, Siekmann AF, Lawson N, Leach SD. Notch-responsive cells initiate the secondary transition in larval zebrafish pancreas. Mech Dev. 2009; 126:898–912. [PubMed: 19595765]

Quillien A, Moore JC, Shin M, Siekmann AF, Smith T, Pan L, Moens CB, Parsons MJ, Lawson ND. Distinct Notch signaling outputs pattern the developing arterial system. Development. 2014; 141:1544–1552. [PubMed: 24598161]

Rhodes J, Hagen A, Hsu K, Deng M, Liu TX, Look AT, Kanki JP. Interplay of pu.1 and gata1 determines myelo-erythroid progenitor cell fate in zebrafish. Dev Cell. 2005; 8:97–108. [PubMed: 15621533]

Robert-Moreno A, Guiu J, Ruiz-Herguido C, Lopez ME, Ingles-Esteve J, Riera L, Tipping A, Enver T, Dzierzak E, Gridley T, et al. Impaired embryonic haematopoiesis yet normal arterial development in the absence of the Notch ligand Jagged1. EMBO J. 2008; 27:1886–1895. [PubMed: 18528438]

Roca FJ, Mulero I, Lopez-Munoz A, Sepulcre MP, Renshaw SA, Meseguer J, Mulero V. Evolution of the inflammatory response in vertebrates: fish TNF-alpha is a powerful activator of endothelial cells but hardly activates phagocytes. J Immunol. 2008; 181:5071–5081. [PubMed: 18802111]

Sainson RC, Johnston DA, Chu HC, Holderfield MT, Nakatsu MN, Crampton SP, Davis J, Conn E, Hughes CC. TNF primes endothelial cells for angiogenic sprouting by inducing a tip cell phenotype. Blood. 2008; 111:4997–5007. [PubMed: 18337563]

Santoro MM, Samuel T, Mitchell T, Reed JC, Stainier DY. Birc2 (cIap1) regulates endothelial cell integrity and blood vessel homeostasis. Nat Genet. 2007; 39:1397–1402. [PubMed: 17934460]

Shalaby MR, Sundan A, Loetscher H, Brockhaus M, Lesslauer W, Espevik T. Binding and regulation of cellular functions by monoclonal antibodies against human tumor necrosis factor receptors. J Exp Med. 1990; 172:1517–1520. [PubMed: 2172437]

Shin HM, Minter LM, Cho OH, Gottipati S, Fauq AH, Golde TE, Sonenshein GE, Osborne BA. Notch1 augments NF-kappaB activity by facilitating its nuclear retention. EMBO J. 2006; 25:129–138. [PubMed: 16319921]

Song LL, Peng Y, Yun J, Rizzo P, Chaturvedi V, Weijzen S, Kast WM, Stone PJ, Santos L, Loredo A, et al. Notch-1 associates with IKKalpha and regulates IKK activity in cervical cancer cells. Oncogene. 2008; 27:5833–5844. [PubMed: 18560356]

Stein SJ, Baldwin AS. Deletion of the NF-kappaB subunit p65/RelA in the hematopoietic compartment leads to defects in hematopoietic stem cell function. Blood. 2013; 121:5015–5024. [PubMed: 23670180]

Takizawa H, Boettcher S, Manz MG. Demand-adapted regulation of early hematopoiesis in infection and inflammation. Blood. 2012; 119:2991–3002. [PubMed: 22246037]

Thisse C, Thisse B, Schilling TF, Postlethwait JH. Structure of the zebrafish snail1 gene and its expression in wild-type, spadetail and no tail mutant embryos. Development. 1993; 119:1203–1215. [PubMed: 8306883]

van der Vaart M, van Soest JJ, Spaink HP, Meijer AH. Functional analysis of a zebrafish myd88 mutant identifies key transcriptional components of the innate immune system. Dis Model Mech. 2013; 6:841–854. [PubMed: 23471913]

Wang H, Tian Y, Wang J, Phillips KL, Binch AL, Dunn S, Cross A, Chiverton N, Zheng Z, Shapiro IM, et al. Inflammatory cytokines induce NOTCH signaling in nucleus pulposus cells: implications in intervertebral disc degeneration. J Biol Chem. 2013; 288:16761–16774. [PubMed: 23589286]

Westerfield, M. A guide for the laboratory use of zebrafish (Danio rerio). 4. Univ. of Oregon Press; Eugene: 2000. The Zebrafish Book.

Wiens GD, Glenney GW. Origin and evolution of TNF and TNF receptor superfamilies. Dev Comp Immunol. 2011; 35:1324–1335. [PubMed: 21527275]

Wynn TA, Chawla A, Pollard JW. Macrophage biology in development, homeostasis and disease. Nature. 2013; 496:445–455. [PubMed: 23619691]

Zhao C, Xiu Y, Ashton J, Xing L, Morita Y, Jordan CT, Boyce BF. Noncanonical NF-kappaB signaling regulates hematopoietic stem cell self-renewal and microenvironment interactions. Stem cells. 2012; 30:709–718. [PubMed: 22290873]

Zhao JL, Ma C, O'Connell RM, Mehta A, Diloreto R, Heath JR, Baltimore D. Conversion of Danger Signals into Cytokine Signals by Hematopoietic Stem and Progenitor Cells for Regulation of Stress-Induced Hematopoiesis. Cell stem cell. 2014

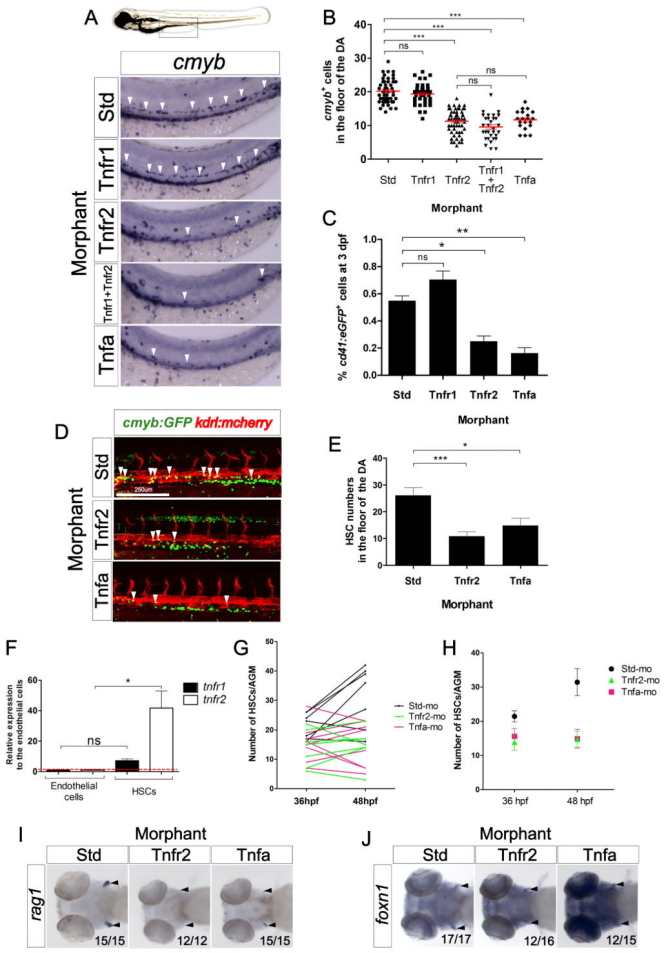

Figure 1. Tnfa and Tnfr2 are required for HSC generation

(A) Standard control (Std), Tnfr1, Tnfr2, Tnfa, and Tnfr1 and Tnfr2 morphants were examined by WISH for *cmyb* expression in the aortic floor at 48hpf. White arrowheads denote *cmyb*$^+$ HSPCs. **(B)** Quantification of *cmyb*$^+$ HSPCs from (A). Each dot represents total *cmyb*$^+$ cells per embryo. The mean ± S.E.M. for each group of embryos is shown in red. **(C)** *cd41:eGFP* transgenic embryos were injected with Std, Tnfr1, Tnfr2, and Tnfa MOs and subjected to flow cytometric analysis at 3dpf. Each bar represents the percentage of *cd41*:GFP$^+$ cells in each sample and is the mean ± S.E.M of 3–7 independent samples of 5 embryos each. **(D)** Maximum projections of 48hpf *cmyb:eGFP; kdrl:memCherry* double transgenic embryos injected with Std, Tnfr2, and Tnfa MOs. Arrowheads denote *cmyb*$^+$, *kdrl*$^+$ HSCs along the DA. All views: anterior to left. **(E)** Enumeration of *cmyb*$^+$, *kdrl*$^+$ HSCs shown in (D). Bars represent mean ± S.E.M of Std (n=13), Tnfr2 (n=13), and Tnfa (n=8) morphants. **(F)** *cmyb*$^-$, *kdrl*$^+$ endothelial cells and *cmyb*$^-$, *kdrl*$^+$ HSCs were isolated from *cmyb:GFP; kdrl:mcherry* transgenic fish by FACS at 48hpf and examined for expression of *tnfr1* and *tnfr2*. Bars represent means ± S.E.M. of two biological replicates. **(G)** Confocal tracking of HSC numbers in the floor of the DA from individual *cmyb:eGFP; kdrl:mcherry* transgenic animals at 36 and 48 hpf following depletion of Tnfr2 or Tnfa compared to standard control morphants. **(H)** Means ± S.E.M. of cmyb$^+$ cell numbers from (G). **(I–J)**

WISH for the T lymphocyte and thymic epithelial markers *rag1* (I) and *foxn1* (J) (black arrowheads), respectively, in Tnfr2 and Tnfa morphants compared to Std controls at 4 dpf. All views are ventral, with anteriors to left. Numbers represent embryos with displayed phenotype; ns, not significant; *p<0.05, **p<0.01, ***p<0.001. See also Supplementary Figure 1.

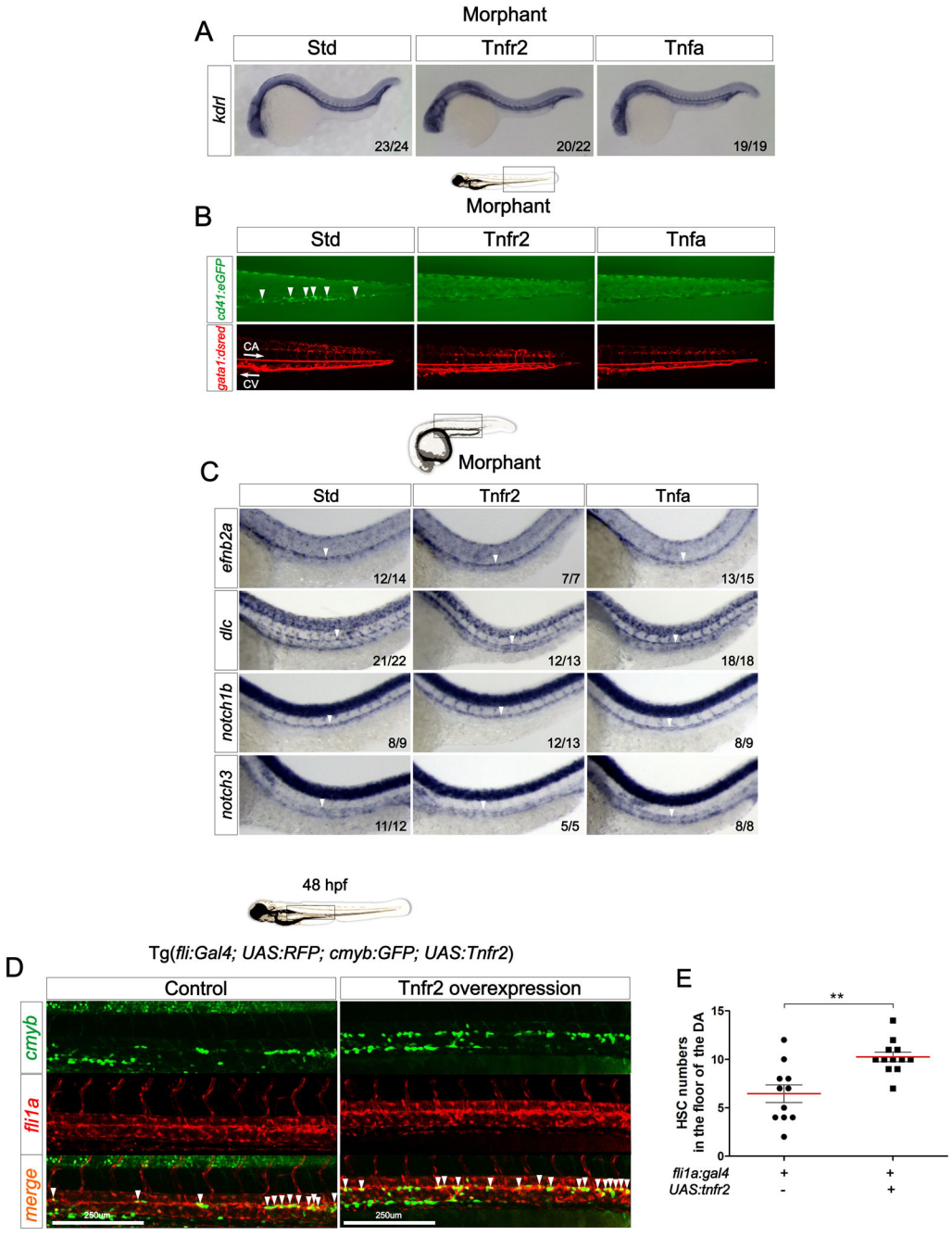

Figure 2. Signaling through Tnfr2 regulates HSC development independently of its role in vascular formation

(A) Std, Tnfr2, and Tnfa morphants were interrogated by WISH for the expression of *kdrl* at 24hpf. **(B)** *cd41:*eGFP*; gata1a:*dsred double transgenic embryos were injected with Std, Tnfr2, and Tnfa MOs and visualized at 3dpf. Arrowheads indicate *cd41*:GFP^{+} HSPCs in the CHT located between the caudal artery (CA) and caudal vein (CV). Arrows indicate blood flow direction. **(C)** Expression of the arterial markers *efnb2a*, *dlc*, *notch1b*, and *notch3* in Std, Tnfr2, and Tnfa morphants analyzed by WISH at 28hpf. Arrowheads denote the CA. **(D)** Maximum projections of *fli1a:Gal4; UAS:tnfr2; cmyb:eGFP; kdrl:memCherry*

transgenic embryos at 48hpf. Region shown includes the DA, and arrowheads denote *cmyb*$^{+}$; *kdrl*$^{+}$ HSCs. **(E)** Enumeration of *cmyb*$^{+}$; *kdrl*$^{+}$ HSCs shown in (D). Each dot is the number of *kdrl*$^{+}$*; cmyb*$^{+}$ cells per embryo. Means ± S.E.M. for each group is shown in red. **p<0.01. All views are lateral, with anteriors to the left. Numbers in panels represent larvae with indicated phenotype. See also Supplementary Figure 2.

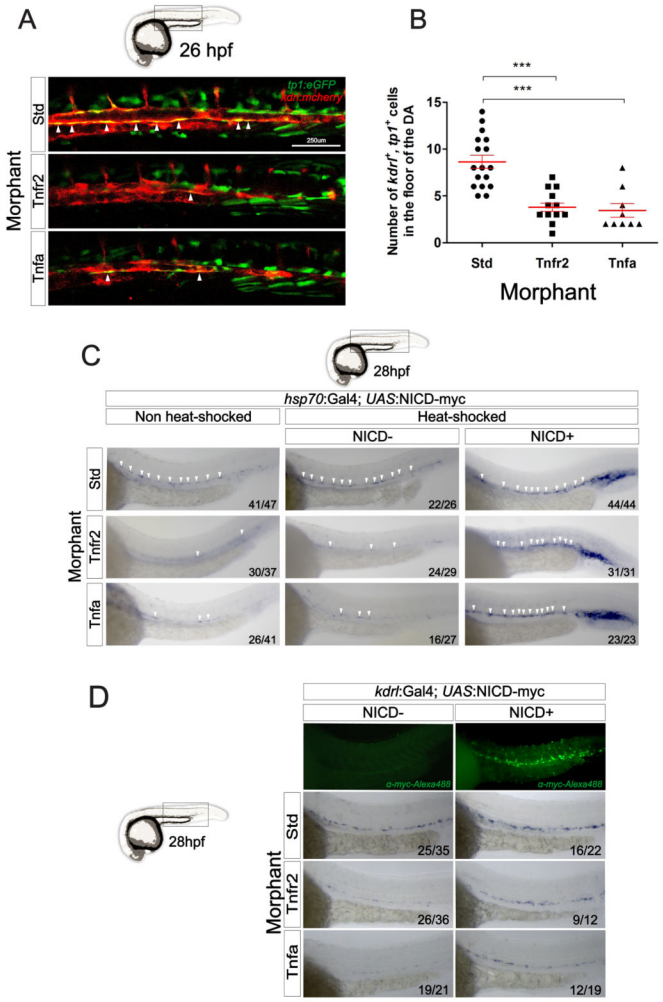

Figure 3. Tnfa and Tnfr2 act upstream of Notch signaling during HSC specification

(A) *tp1:eGFP; kdrl:mcherry* embryos injected with Std, Tnfr2, and Tnfa MOs were visualized at 26hpf. Arrowheads indicate cells in the floor of the DA with active Notch signaling. **(B)** Enumeration of *tp1*$^{+}$, *kdrl*$^{+}$ HSCs from (A). Each dot represents the number of HSCs per embryo, and red lines indicate means ± S.E.M. ***p<0.001. **(C)** *hsp70:Gal4; UAS:NICD-myc* embryos injected with Std, Tnfr2, and Tnfa MOs were heat-shocked at 18hpf and WISH for *runx1* was performed at 28hpf. Arrowheads denote HSCs along the DA. **(D)** *kdrl:Gal4; UAS:NICD-myc* embryos injected with Std, Tnfr2, and Tnfa MOs were analyzed by WISH for *runx1* at 28hpf. NICD^{+} larvae were identified using anti-myc-Alexa488 antibody (top panel). Numbers in panels represent the numbers of larvae with indicated phenotype.

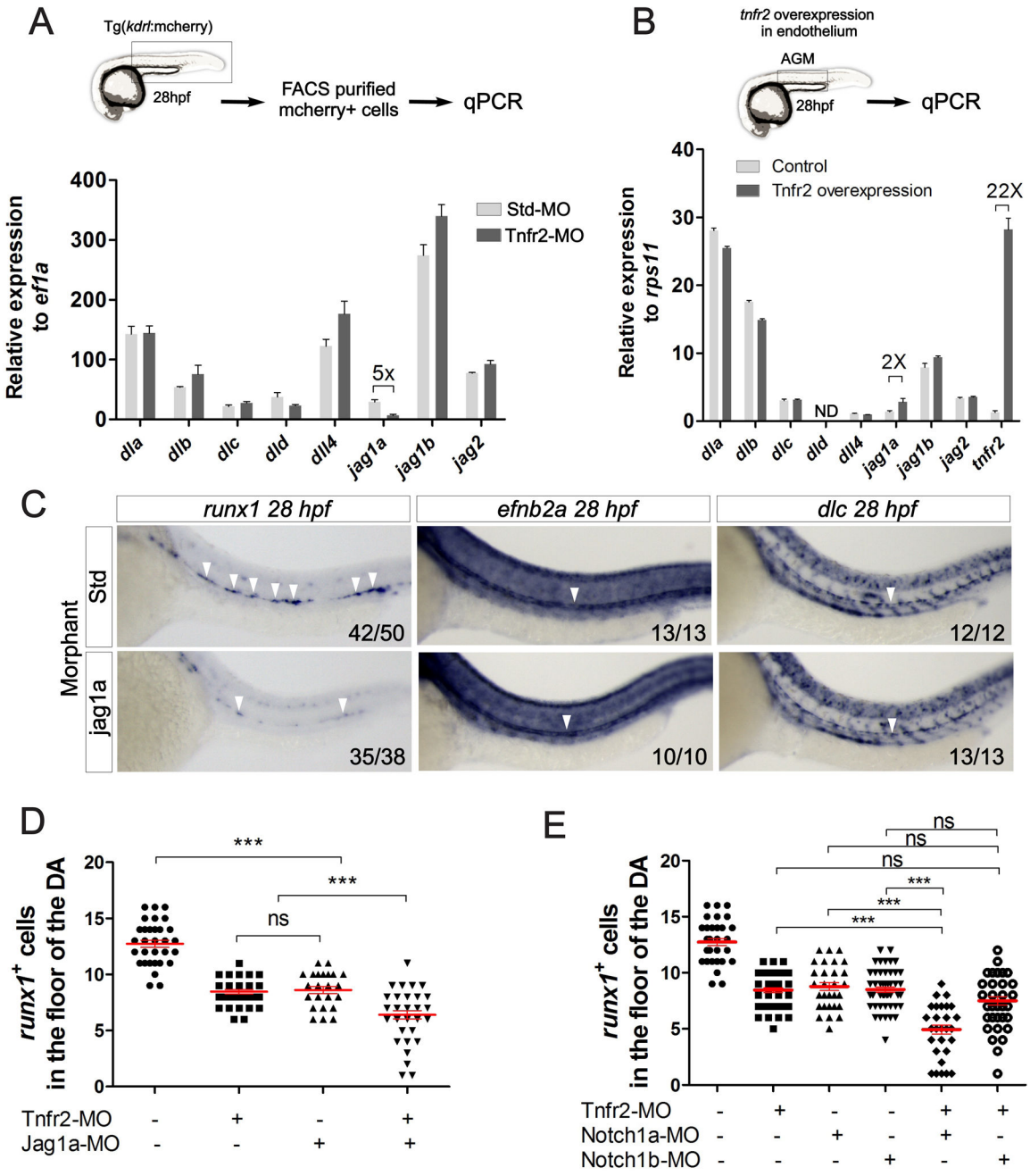

Figure 4. Tnfr2 induces *jagged1a* in endothelial cells, encouraging HSC specification

(A) *kdrl:mcherry*$^{+}$ cells from dissected trunks of Std or Tnfr2 morphants were purified by FACS at 28hpf for qPCR. Levels of indicated transcripts along x-axis are shown relative to the housekeeping gene *ef1a*. Bars represent means ± S.E.M. of duplicate samples. **(B)** AGM regions from *fli1a:Gal4; UAS:Tnfr2* embryos were dissected and subjected to qPCR for transcripts shown along x-axis. Bars represent means ± S.E.M. of expression relative to the housekeeping gene *rps11*. **(C)** Std (top panels) or Jag1a (bottom panels) morphants were interrogated for *runx1* expression at 26hpf and *efnb2a* and *dlc* at 28hpf by WISH. Numbers represent larvae with indicated phenotype. **(D)** Enumeration of *runx1*$^{+}$ cells in Tnfr2 and/or

Jag1a morphants at 28hpf. **(E)** Enumeration of *runx1*$^{+}$ cells in Tnfr2 and/or Notch1a and/or Notch1b morphants at 28hpf. Each dot is the number of HSCs per embryo, and red lines indicate means ± S.E.M. (D–E) ***p<0.001; ns, not significant. See also Supplementary Figure 3.

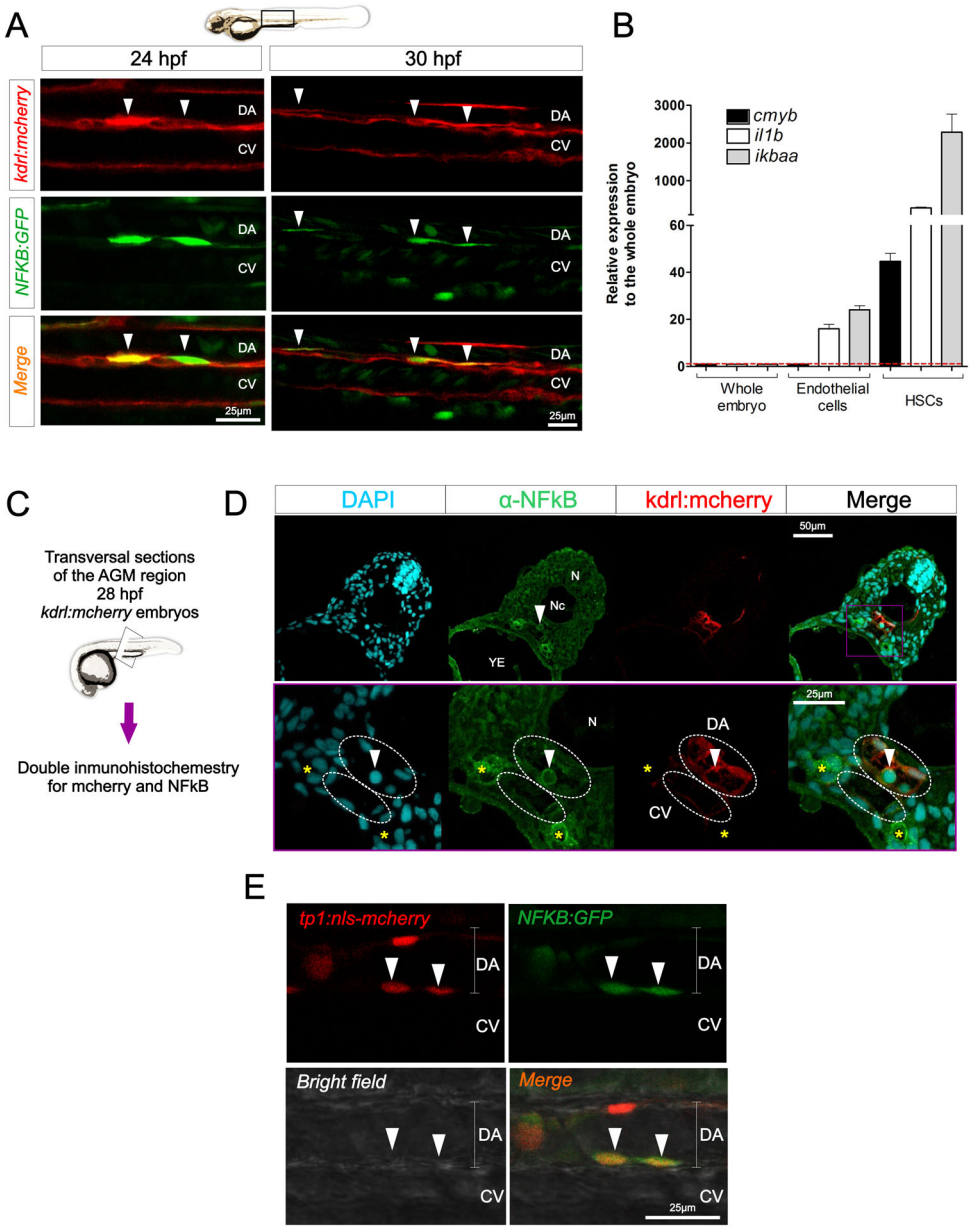

Figure 5. NF-κB is active in emerging HSCs

(A) Trunk region of *kdrl:mcherry; NFKB:GFP* double transgenic animals visualized by confocal microscopy at 24hpf (left panels) and 30hpf (right panels). Each image is a 2µm z-slice. Arrowheads denote HSCs. **(B)** *cmyb*$^{-}$, *kdrl*$^{+}$ endothelial cells and *cmyb*$^{+}$, *kdrl*$^{+}$ HSCs were isolated by FACS at 48hpf. Levels of the NF-κB target genes *ikbaa* and *il1b*, as well as the HSC marker *cmyb* are shown relative to *ef1a*. Bars represent means ± S.E.M. of two biological replicates. **(C)** Schematic representation of the experimental design of (D). 28hpf *kdrl:mcherry* animals were transversally sectioned and subjected to double immunohistochemistry for mcherry (red) and NF-κB (green). DAPI (blue) was added to visualize nuclei. **(D)** Maximum projections of 1µm sections. Arrowhead indicates a potential HSC emerging in the DA. DA and CV are demarcated by dashed white lines. Yellow

asterisks indicate pronephric ducts. **(E)** *tp1:nls-mcherry; NFKB:GFP* animals were visualized by confocal microscopy at 24hpf. Each image is a 2μm z-slice. Arrowheads indicate HSCs. CV, caudal vein; DA, dorsal aorta; N, neural tube; Nc, notochord; YE, yolk extension. See also Supplementary Video 1.

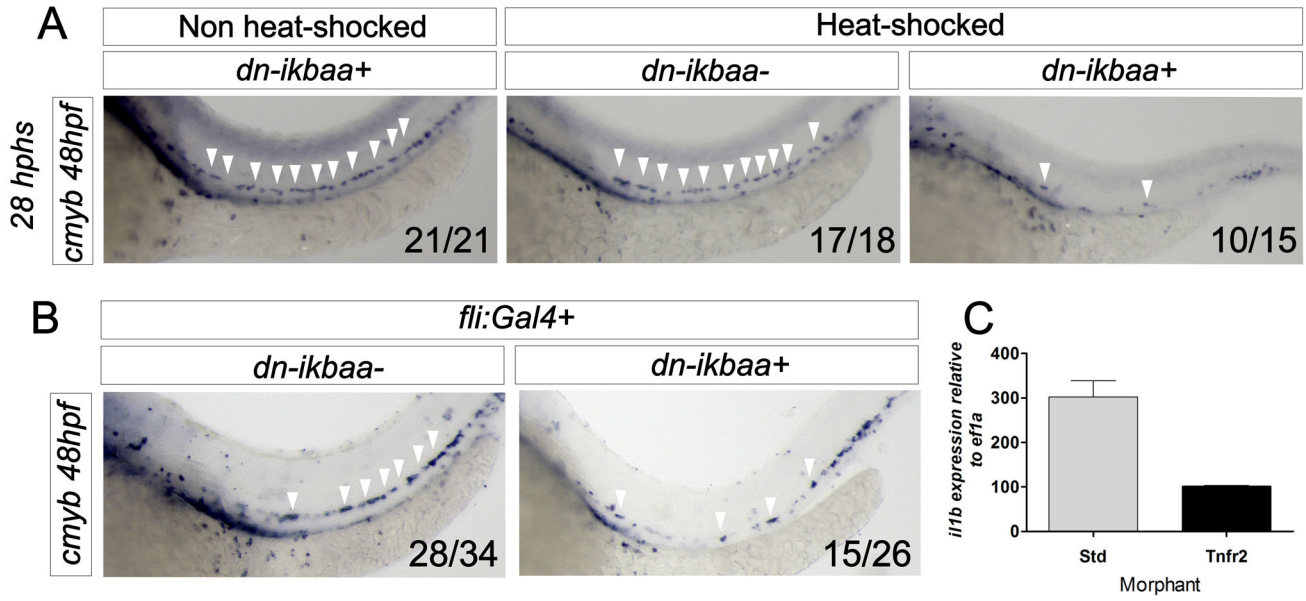

Figure 6. NF-κB is required for HSC specification and acts downstream of Tnfr2

(A) *hsp70:Gal4; UAS:dn-ikbaa* embryos were heat-shocked at 20 hpf. WISH for *cmyb* was performed at 48hpf. **(B)** WISH for *cmyb* in *fli1:Gal4; UAS:dn-ikbaa*$^{-}$ (left) and *fli1:Gal4; UAS:dn-ikbaa*$^{+}$ (right) embryos. Arrowheads mark *cmyb*$^{+}$ cells along the DA. **(C)** *kdrl:mcherry*$^{+}$ cells were FACS sorted from Std or Tnfr2 morphants at 28hpf for qPCR. Levels of the NF-κB target gene *il1b* are shown relative to *ef1a*. Bars represent means ± S.E.M. from duplicate samples. See also Supplementary Figure 4.

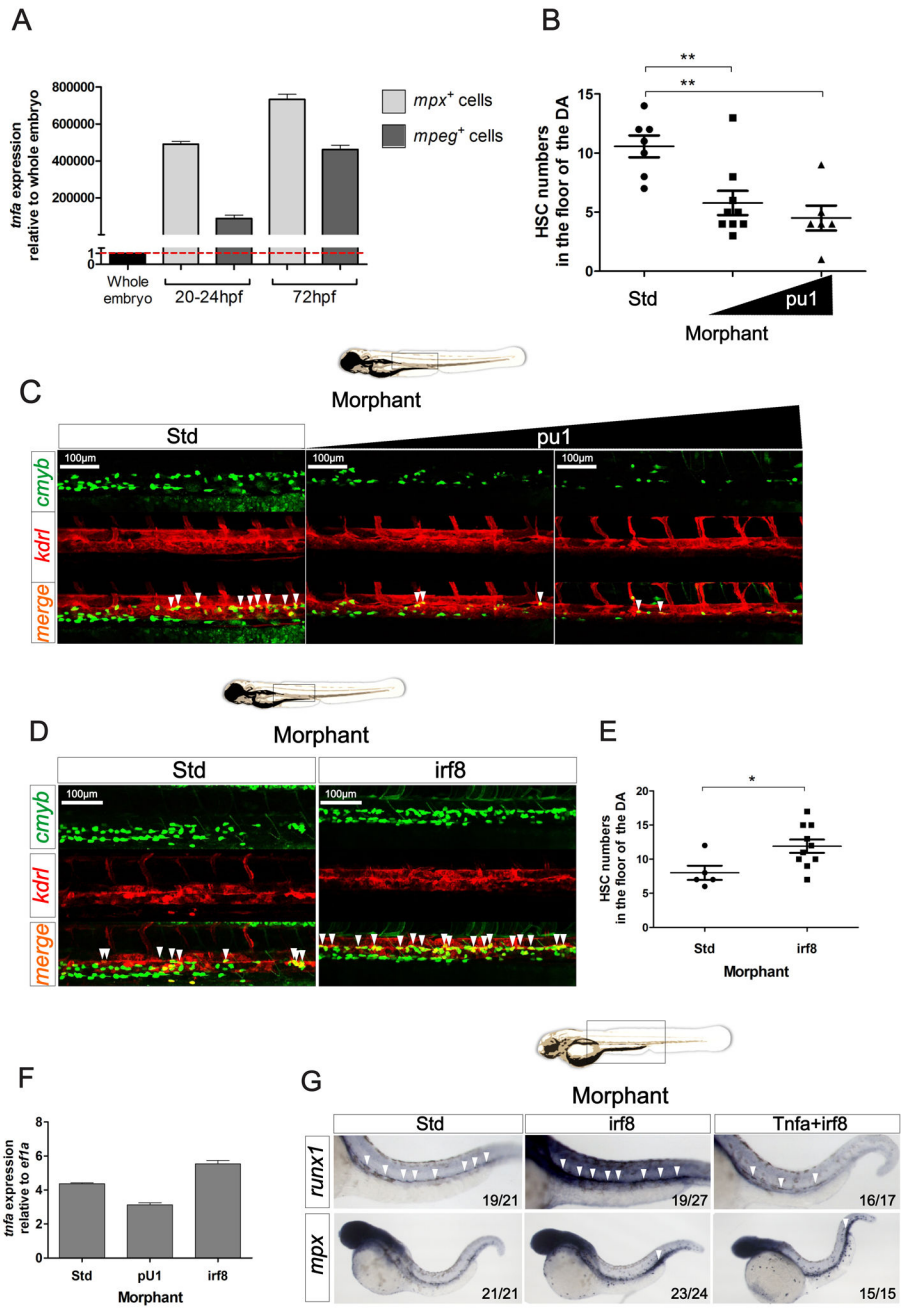

Figure 7. Primitive myeloid cells play a key role in HSC specification

(A) Primitive neutrophils (*mpx:GFP*$^+$) and macrophages (*mpeg:GFP*$^+$) were isolated at 20–24 and 72 hpf by FACS and *tnfa* expression was quantified by qPCR. Expression was normalized to *ef1a* and is presented relative to whole embryo expression. Bars represent means ± S.E.M. of two independent experiments. **(B)** Enumeration of *cmyb*$^+$; *kdrl*$^+$ HSCs shown in (C). **(C)** Maximum projections of representative images of *cmyb:eGFP; kdrl:m Cherry* embryos at 48hpf following injections of Std or pU.1 MOs, the latter at two different concentrations. Region shown is the DA, and arrowheads denote *cmyb*$^+$; *kdrl*$^+$ HSCs. **(D)** Maximum projections of representative images of *cmyb:eGFP; kdrl:memCherry* embryos at

48hpf in Std and irf8 morphants. Arrowheads denote *cmyb*$^{+}$; *kdrl*$^{+}$ HSCs. **(E)** Enumeration of *cmyb*$^{+}$; *kdrl*$^{+}$ HSCs shown in (D). **(F)** *tnfa* expression relative to *ef1a* in 28hpf Std, pU.1 or irf8 morphants. Bars represent means ± S.E.M of duplicate samples. **(G)** Std, irf8, and irf8+Tnfa morphants were interrogated by WISH for *runx1* and *mpx* at 28hpf. All views are lateral, with anteriors to the left. Numbers represent larvae with indicated phenotypes. *p<0.05; ***p<0.001. See also Supplementary Figure 5.